Article

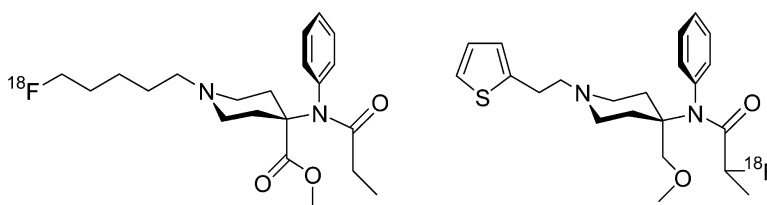# Syntheses, Biological Evaluation, and Molecular Modeling of F-Labeled 4-Anilidopiperidines as □-Opioid Receptor Imaging Agents

Gjermund Henriksen, Stefan Platzer, Jnos Marton, Andrea Hauser, Achim Berthele, Markus Schwaiger, Luciana Marinelli, Antonio Lavecchia, Ettore Novellino, and Hans-Jrgen Wester

More About This Article

Additional resources and features associated with this article are available within the HTML version:

- Supporting Information
- Links to the 2 articles that cite this article, as of the time of this article download
- Access to high resolution figures
- Links to articles and content related to this article
- Copyright permission to reproduce figures and/or text from this article

View the Full Text HTML

Syntheses, Biological Evaluation, and Molecular Modeling of ^{18}F-Labeled 4-Anilidopiperidines as *μ*-Opioid Receptor Imaging Agents

Gjermund Henriksen,[†,*] Stefan Platzer,[‡] János Marton,[§] Andrea Hauser,[†] Achim Berthele,[‡] Markus Schwaiger,[†] Luciana Marinelli,[⊥] Antonio Lavecchia,[⊥] Ettore Novellino,[⊥] and Hans-Jürgen Wester[†]

Department of Nuclear Medicine, Klinikum rechts der Isar, Technische Universität München, Ismaninger Strasse 22, D-81675 Munich, Germany, Department of Neurology, Klinikum rechts der Isar, Technische Universität München, Möhlstrasse 28, D-81675 Munich, Germany, ABX Advanced Biochemical Compounds GmbH, Heinrich-Glaeser-Strasse 10-14, D-01454 Radeberg, Germany, and Dipartimento di Chimica Farmaceutica e Tossicologica, Università di Napoli "Federico II", Via D. Montesano, 49-80131 Napoli, Italy

The synthesis, evaluation, and molecular modeling of a series of ^{18}F-labeled 4-anilidopiperidines with high affinities for the *μ*-opioid receptor (*μ*-OR) are reported. On the basis of the high brain uptake and selective retention in brain regions that contain a high concentration of the *μ*-OR, combined with a good metabolic stability, [^{18}F]fluoro-pentyl carfentanil ([^{18}F]**4**) and 2-(±)[^{18}F]-fluoropropyl-sufentanil ([^{18}F]**6**) were selected as the lead compounds for further evaluation. The binding affinity to the human *μ*-OR was 0.74 and 0.13 nM for [^{18}F]**4** and [^{18}F]**6**, respectively. In vitro autoradiography of [^{18}F]**4** and [^{18}F]**6** on rat brain sections produced patterns in accordance with the known distribution of *μ*-OR expression. Structure−activity relationships of the fluorinated compounds are discussed with respect to the interaction with an activated-state model of the *μ*-OR. Taken together, the in vivo and in vitro data indicate that [^{18}F]**4** and [^{18}F]**6** hold promise for studying the *μ*-opioid receptor in humans by means of positron emission tomography.

Introduction

The opioid receptors (ORs) belong to the superfamily of G protein-coupled receptors (GPCRs) that produce their effects by activation of intracellular G proteins. The *μ*-opioid receptor (*μ*-OR) is one of three classes of ORs and plays an important role in the modulation of nociceptive signaling encountered in stress-induced analgesia, in analgesic placebo effect and in the actions of exogenously administered opiate drugs.[1−4] Alterations in *μ*-opioidergic neuronal function in man has been shown to be involved in addiction-related phenomena, such as cocaine-[5] and alcohol craving.[6] A role of the *μ*-OR can be inferred for anxiety and affection related disorders.[7] Despite its prominent function in several clinically relevant diseases and syndromes, the precise role of the *μ*-OR and their ligands in humans is incompletely understood.

PET-imaging of receptors in the central nervous system in humans provides a useful tool to understand how opioid receptor density and occupancy are related to function.[8−11] At present, [^{11}C]carfentanil ([^{11}C]Caf; ^{11}C: $t_{1/2}$ = 20.3 min) is the only available radioligand for positron emission tomography (PET) imaging of *μ*-OR in humans. It shows high *μ*-OR affinity and high selectivity over *κ*- and *δ*-OR, and its specific binding in vivo correlates with the known density of *μ*-OR in the human brain.[3,4] Despite being frequently used, [^{11}C]Caf has several limitations. Its potent agonistic activity

requires labeling at very high specific activities to ensure administration in subpharmacological doses.[3] For an imaging protocol where 740 MBq is administered, a specific activity ≥ 88 GBq/*μ*mol (2.38 Ci/*μ*mol) at the time of injection is indispensable. Furthermore, a radiotracer based on carbon-11 allows sufficient counting statistics only for relatively short-lasting imaging protocols. Thus, applicability of [^{11}C]Caf for longer acquisition times is limited to the use of a bolus + infusion protocol which, due to an increase in the concentration of pharmacological active carfentanil, imposes less safety of the application. To improve the feasibility of a full kinetic data analysis and to provide useful alternative PET tracers, ^{18}F-fluorinated ($t_{1/2}$ = 109.7 min) *μ*-OR selective compounds are of interest for investigation. Compared to ^{11}C-labeled tracers they would imply applicability to more flexible experimental designs, including the use of single bolus protocols in displacement studies, i.e., where the PET-ligand is competing with endogenously released ligands or administered drugs.

Compounds belonging to the 4-anilidopiperidine (4-AP) series have been shown to preferentially increase *μ*-OR occupancy and subsequent signaling. The 4-APs alfentanil, carfentanil, fentanyl, remifentanil, and sufentanil (Chart 1) are potent *μ*-OR agonists and have been extensively explored as pain relieving agents. To date, several analogues with variations of the 4-AP structure have been synthesized and characterized,[12] providing compounds with a wide range of *μ*-OR affinity, selectivity, and pharmacological potency.[13] Thus, the 4-AP may represent optimal leads for the development of ^{18}F-labeled *μ*-OR selective ligands. Existing structure−activity relationships (SARs) of 4-AP derivatives indi-
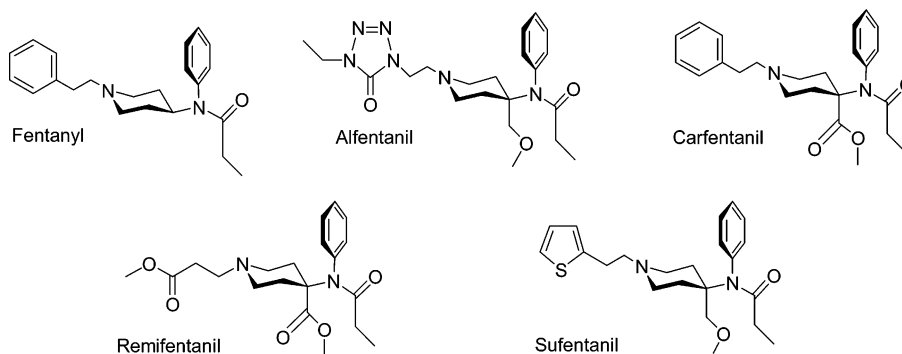
---

* To whom correspondence should be addressed. Tel: + 49 89 4140 6332. Fax: + 49 89 4140 4841. E-mail: G.Henriksen@lrz.tum.de.
　† Department of Nuclear Medicine, Technische Universität München.
　‡ Department of Neurology, Technische Universität München.
　§ ABX Advanced Biochemical Compounds GmbH.
　⊥ Università di Napoli "Federico II".

Chart 1. Selected 4-Anilidopiperidines

**Scheme 1.** Syntheses of Fluorinated 4-Anilidopiperidine Derivatives
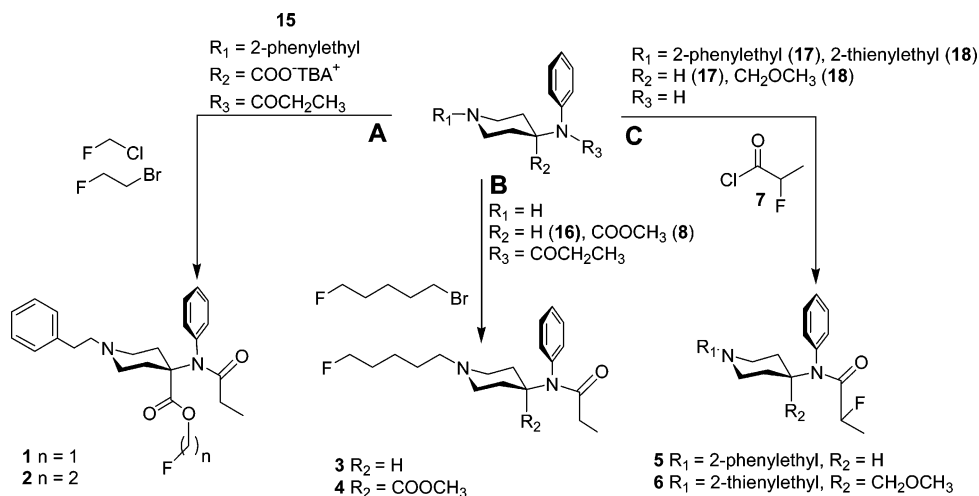
cate a certain flexibility to the selection of the N^1-piperidine substituent for providing potent compounds.[12–14] In contrast, for the alkyl chain group of the *N*-phenylalkyl amide part, as well as for substituents in the 4-axial position, a narrow span of the size is encountered in compounds of high potency.[12–14] We report here the syntheses and the evaluation of a series of ^{18}F-fluorinated-4-APs prepared (Scheme 1) by (A) ^{18}F-fluoroalkylation of the carboxylic acid function of *des*-methyl carfentanil, (B) N^1-^{18}F-fluoropentylation of *des*-phenethyl analogues and (C) ^{18}F-fluoroacylation of *des*-propionyl 4-AP precursors. The effects of fluorine substitution on the properties of 4-APs have been systematically investigated, and structural requirements determining the applicability of the compounds in PET (e.g. properties governing brain uptake, metabolism, and regional brain uptake kinetics) have been established. To rationalize the SARs of the ^{18}F-fluorinated compounds, flexible docking of compound **6** into an active state model of μ-opioid receptor [15] was carried out.

Result and Discussion

Synthesis and Radiolabeling. Three different approaches were followed for providing fluoro-4-AP reference compounds (Scheme 1) and their ^{18}F-labeled versions (Scheme 2). In approach A (Scheme 1), fluoroalkyl esters analogues of carfentanil were obtained by treatment of carfentanil carboxylic acid **15** with fluoroalkylating agents. In approach B, the two 4-AP-carboxamides *nor*-fentanyl **16** and *nor*-carfentanil **8** were

transformed into the N^1-5-fluoropentyl 4-APs **3** and **4**, respectively, by N^1-piperidine amine-alkylation with 5-fluoropentyl bromide. By the third approach (C), the reaction of ($\pm$)2-fluoropropionyl chloride with *des*-propionylfentanyl **17** and *des*-propionyl sufentanil **18** gave the *N*-anilido-2-fluoropropionyl-4-APs **5** and **6**, respectively.

Representative examples of radiolabeling reactions to produce [^{18}F]fluoroalkyl esters (2-[^{18}F]fet-Caf; [^{18}F]**2**), N^1-piperidine-[^{18}F]fluoroalkylated compounds ([^{18}F]fpe-Caf; [^{18}F]**4**), and *N*-anilido-($\pm$)2-[^{18}F]fluoropropionyl compounds ([^{18}F]fpr-Suf; [^{18}F]**6**) are shown in Scheme 2 (see Experimental Section for details). The described strategies to ^{18}F-labeled 4-APs were selected according to their potential for automation and large-scale production under clinical settings. Thus, the ease of syntheses, an efficient ^{18}F-fluorination of secondary precursors, efficient and fast transformations to the final product including purification steps had to be considered. In approach A, carfentanil carboxylate was transformed to the [^{18}F]fluoromethyl ester using [^{18}F]fluoromethyl bromide [42a] and to the [^{18}F]fluoroethyl ester using [^{18}F]-fluoroethyl tosylate ($\sim$30% radiochemical yield (RCY).[42b] [^{18}F]**3** and [^{18}F]**4** as members of the second group of tracers (Scheme 2, B), were generated by N^1-alkylation of *des*-phenethylfentanyl and -carfentanil, respectively, using [^{18}F]fluoropentyl bromide with sodium iodide as catalyst ($\sim$57% RCY). ^{18}F-Fluoropropionylation of *des*-propionylfentanyl and -sufentanil (Scheme 2, C) resulted in the corresponding radiolabeled products [^{18}F]**5** and [^{18}F]**6** possessing a formal F-for-H-substitution in the

Scheme 2. Examples of ^{18}F-Radiolabeling Reactions with ^{18}F-Fluoroalkylation and ^{18}F-Fluoroacylation Agents
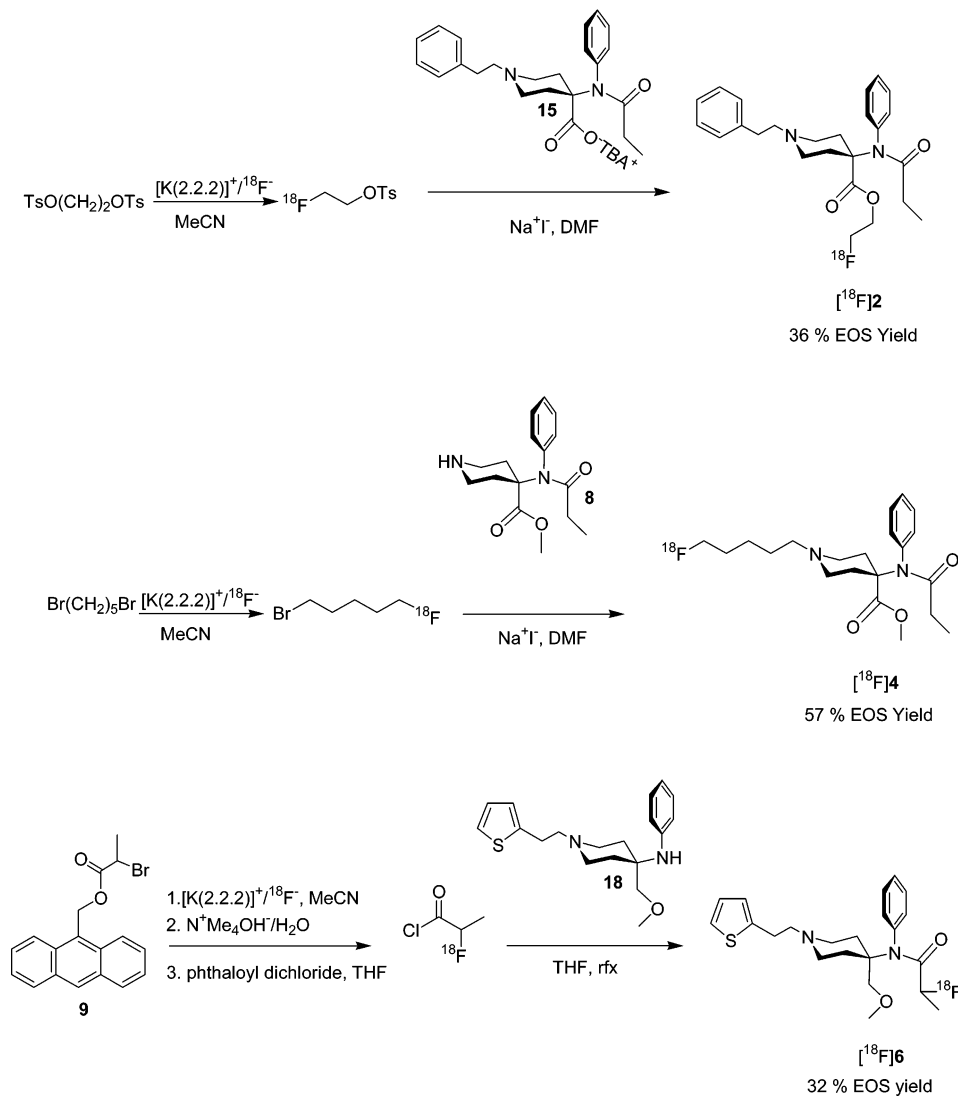
Scheme 3. Synthesis of *nor*-Carfentanil (**8**)^a
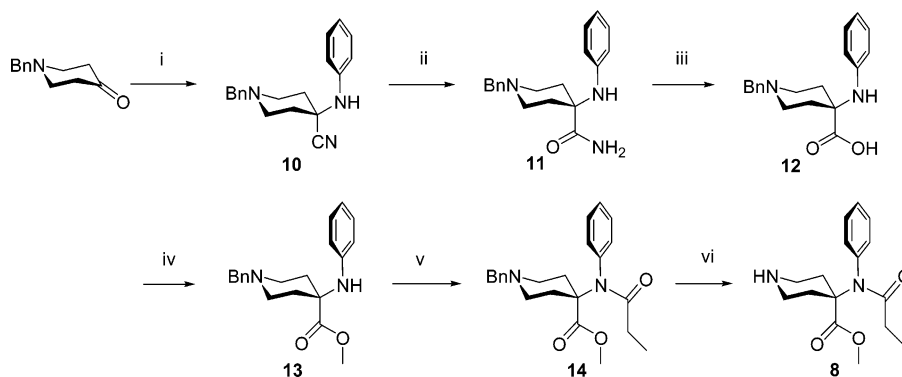
^{a} Reagents and conditions *i*: KCN, PhNH$_2$, AcOH; *ii*: 1. H$_2$SO$_4$, 2. NH$_4$OH; *iii*: KOH, 1,2-ethanediol, 190 °C; *iv*: NaH, absol DMF, MeI; *v*: (EtCO)$_2$O, reflux; *vi*: H$_2$, Pd/C, EtOH.
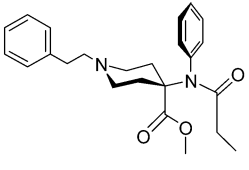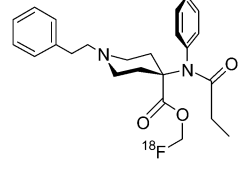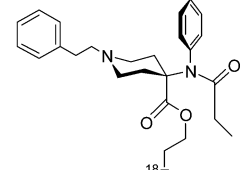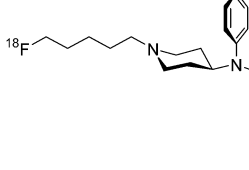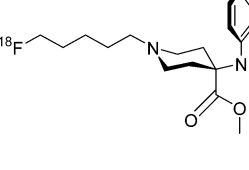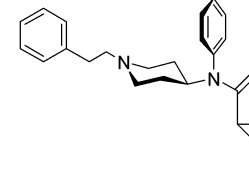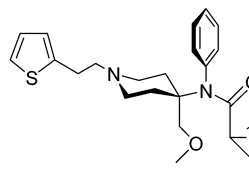
acyl chain (∼32% RCY). These derivatives, together with [^{18}F]fluoromethylcarfentanil, represent the three ^{18}F-compounds with the highest structural similarity relative to their native counterparts.

Although the yields of the respective radiosyntheses are not optimized, all compounds were obtained in an isolated RCY of >30% at end-of-syntheses (EOS) and thus in amounts sufficient for ensuring further evalu-

ation as well as initial patient studies. Although the starting activity of [^{18}F]fluoride for all syntheses was <7.4 GBq at end-of-bombardment, the specific activities obtained were >37 GBq/μmol. All syntheses were completed in less than 2 h after EOB and were carried out using a semiautomated remote controlled apparatus.

Octanol/Water Partition Coefficient and Biological Evaluation. To correlate the brain uptake of

Table 1. Lipophilicity, μ-Opioid Receptor Binding Affinities, and Brain Uptake (% dose/g) in Mice of Fluorinated 4-Anilidopiperidines

compound	log $P_{oct/PBS}$[a]	K_i (nM)[b]	total brain uptake[a]		
			5 min	20 min	60 min
[11C]Caf	3.58±0.03	0.07±0.04	3.78±0.44	2.42±0.37	1.41±0.24
[18F]**1**	3.62±0.05	0.13±0.05	3.69±1.69	1.27±0.46	0.33±0.08
[18F]**2**	3.75±0.04	1.2±0.3	3.72±0.93	1.63±0.67	1.11±0.34
[18F]**3**	2.14±0.03	13.5±2.2	2.83±0.61	1.58±0.49	0.95±0.36
[18F]**4**	2.42±0.04	0.74±0.52	3.31±0.65	2.11±0.44	1.27±0.28
[18F]**5**	2.90±0.02	2.1±0.6	3.31±0.75	1.90±0.39	1.07±0.28
[18F]**6**	3.32±0.04	0.13±0.05	4.48±0.82	2.38±0.42	1.38±0.35

[a] The results represent the means ± SD, $n = 3-4$. [b] Measured by competition binding studies to the cloned human μ-opioid receptor.

the compounds investigated in mice, the octanol–water partition coefficients (log $P_{oct/PBS}$) were determined (Table 1). Generally, a value of log $P_{oct/PBS}$ in the range of 2–3[49] is required in order to have a brain uptake suitable for in vivo imaging. The log $P_{oct/PBS}$ values of the 4-AP derivatives investigated ([18F]**1**–**6**) were within a range of 2.14 ± 0.04 ([18F]**3**) and 3.75 ± 0.04 ([18F]**2**). The measure of the lipophilicity of the compounds roughly correlate with their brain uptake 5 min postinjection (pi) (Table 1). The initial uptake of [18F]**1**, [18F]-**2**, [18F]**4**, [18F]**5**, [18F]**6** is comparable to that of successful tracers used for opioid receptor imaging in PET includ-
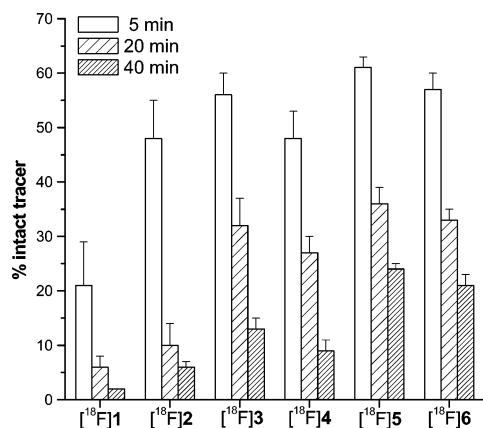
Figure 1. Percent intact compound in plasma of mice as function of time (mean ± SD, n = 3, 4).

ing [^{11}C]Caf[16] (3.73 ± 0.34% ID/g at 5 min pi),[17] and the nonspecific ($K_{D,\mu} \sim K_{D,\delta} \sim K_{D,\kappa}$) opioid receptor tracers 6-*O*-[^{11}C-methyl]diprenorphine (7.5 ± 0.89% ID/g at 7 min pi)[18] and 6-*O*-desmethyl-(2-[^{18}F]fluoroethyl diprenorphine (4.36 ± 0.49% ID/g at 5 min pi).[18] [^{18}F]**3**, having the lowest lipophilicity, also showed the lowest brain uptake.

For investigation of the metabolic stability of the tracers after iv injection, compounds [^{18}F]**1**−**6** were injected into male Balb-C mice, and the amount of intact tracer present in plasma was determined by reverse-phase high performance liquid chromatography (RP-HPLC). The peripheral metabolism of all compounds was rapid. Only 21−57% and 2−21% of the total activity in plasma was found to be the intact tracers at 5 and 40 min pi, respectively (Figure 1). Esters [^{18}F]**1** and [^{18}F]-**2** displayed the lowest metabolic stability while compounds [^{18}F]**5** and [^{18}F]**6** displayed the highest ratio. For compounds [^{18}F]**3**−**6**, the ratio of intact tracer to metabolite in plasma is comparable to that found for [^{11}C]-Caf in CD1 mice.[19]

Even though quantitative tracer kinetic modeling in PET enables the use of a ligand whose metabolite(s) cross the blood−brain barrier (BBB) by correcting the dynamic plasma data for the brain uptake of metabolite(s),[20−22] a high metabolic stability in blood or at least a negligible ratio of metabolites to intact tracer in brain is preferable. Thus, criteria for selection of lead compounds may be (a) the absence of significant amounts of labeled metabolites in blood, (b) a low blood−brain-barrier penetration of metabolites into the brain, (c) high stability in brain tissue, (d) fast washout of metabolites after formation from the brain, and (e) low binding of metabolites in the brain. In separate experiments were investigated whether radioactive metabolites were contributing to the activity in brain of mice receiving compounds [^{18}F]**1**−**6**. To characterize and quantify radioactive species, mice were injected with the respective compound, and their brains were removed at 40 min after injection and homogenized. Radiolabeled species were extracted from the homogenate with ≥91% efficiency and analyzed using RP-HPLC. For compounds [^{18}F]**3**−**6**, radioactivity in the extracted supernatants was determined to be ≥93% intact tracer 40 min pi, based on the limits of detection, thus representing a conservative estimate of potential metabolization. These experiments indicate high metabolic stability of the

compounds in brain and negligible BBB permeability and binding of peripherally generated metabolites. On the basis of the results from this study, we conclude that the metabolites of [^{18}F]**3**−**6** may not play an important role on the activity distribution of these tracers in the brain of rodents. In contrast, for mice injected with [^{18}F]-**2** only 46 ± 8% of the activity was identified as intact tracer 40 min pi. For mice injected with [^{18}F]**1**, no metabolite was detected in brain homogenates. On the basis of the high affinity of this compound for the μ-OR (Table 1), the fast clearance of radioactivity from brain of mice injected with [^{18}F]**1** is likely to be related to a fast metabolic degradation, i.e., ester hydrolyses of the compound leading to a short retention of the labeled [^{18}F]CH$_2$FOH in the brain.

Binding affinities (K_i values) of compounds **1**−**6** for human μ-OR determined by displacing [^{3}H]DAMGO are shown in Table 1. Affinities ranged from 0.13 nM to 13.5 nM. Among the available PET-opioid ligands that have been used clinically, the binding dissociation constant (K_d) for their opioid receptor targets ranges from 0.02 to 2.6 nM.[23] Compounds with an affinity within this range therefore remain potentially attractive. Based on this requirement, [^{18}F]**4**−**6** (K_i: [^{18}F]**4**: 0.74 nM, [^{18}F]-**5**: 2.1 nM and [^{18}F]**6**: 0.13 nM) are relevant for further evaluation.

Experiments to assess the regional brain distribution of the radiolabeled derivatives were performed in Balb-C-mice. A necessary requirement for a good μ-OR imaging agent is a selective retention in brain regions that contain a high concentration of the receptor, i.e., striatum, thalamus, and cerebral cortex. The cerebellum contains a very low concentration of μ-OR[24] and may be used as an indicator of nonspecific binding. The uptake values and the region/cerebellum ratios for selected regions are shown in Table 2, and the data indicate a selective enrichment of compounds [^{18}F]**4**−**6** in the regions with a high μ-OR density. In a previous study with mice,[50] we found the selective enrichment of [^{18}F]**6** in striatum over cerebellum at 5 and 30 min pi to be comparable to that of [^{11}C]Caf.

A criterion of suitability for in vivo competition studies is the time required to achieve the maximum activity concentration in high binding regions relative to that in low binding regions. Judged by this parameter [^{18}F]**4** and [^{18}F]**6** stand out as promising compounds with [^{18}F]**6** demonstrating the most rapid enrichment (Table 2). Their relatively fast kinetics of reaching peak uptake ratios is highly desirable for future kinetic modeling studies. Due to the promising properties of [^{18}F]**4** and [^{18}F]**6** in mice brain, their binding properties were further evaluated in vitro autoradiography studies. The radioactivity pattern of rat brain sections incubated with [^{18}F]**4** and [^{18}F]**6** showed highly selective binding to brain regions with high μ-opioid receptors density (Figure 2). Compared to no-carrier-added conditions, treatment with naloxone (blocking of μ-, δ-, and κ-ORs) and sufentanil (blocking of μ-OR) reduced the binding of [^{18}F]**4** and [^{18}F]**6** to the receptor-rich regions down to that seen in receptor-poor regions. Thus, the in vitro competition experiment strongly established that the binding of [^{18}F]**4** and [^{18}F]**6** is directly related to binding to the μ-OR. Furthermore, the autoradiography patterns obtained with [^{18}F]**4** and [^{18}F]**6** are in accordance with

Table 2. Regional Brain Uptake Kinetics (% dose/g) of [^{18}F]**4**−**6** in Mice (mean ± SD, $n = 3$−4)

| region	[^{18}F]**4**			[^{18}F]**5**			[^{18}F]**6**		
	5 min	20 min	40 min	5 min	20 min	40 min	5 min	20 min	40 min
A. Regional Brain Distribution (% dose/g)									
striatum	3.58 ± 0.38	2.13 ± 0.34	1.40 ± 0.27	2.95 ± 0.27	1.74 ± 0.22	1.21 ± 0.34	4.61 ± 0.48	2.38 ± 0.34	1.66 ± 0.21
thalamus	3.64 ± 0.44	2.24 ± 0.28	1.36 ± 0.35	3.25 ± 0.44	1.96 ± 0.19	1.25 ± 0.17	4.72 ± 0.51	2.51 ± 0.29	1.70 ± 0.18
cortex	2.41 ± 0.31	1.52 ± 0.17	1.10 ± 0.24	2.29 ± 0.21	1.86 ± 0.28	1.27 ± 0.09	3.15 ± 0.38	1.69 ± 0.26	1.15 ± 0.15
cerebellum	1.89 ± 0.26	0.87 ± 0.14	0.66 ± 0.07	2.31 ± 0.36	0.95 ± 0.18	0.81 ± 0.12	2.16 ± 0.27	0.92 ± 0.17	0.76 ± 0.08
B. Ratio to Cerebellum									
striatum	1.89 ± 0.33	2.45 ± 0.56	2.12 ± 0.47	1.27 ± 0.23	1.83 ± 0.43	1.49 ± 0.48	2.13 ± 0.34	2.59 ± 0.60	2.18 ± 0.36
thalamus	1.93 ± 0.35	2.58 ± 0.53	2.06 ± 0.57	1.41 ± 0.29	2.06 ± 0.44	1.54 ± 0.31	2.19 ± 0.36	2.73 ± 0.60	2.24 ± 0.33
cortex	1.28 ± 0.24	1.75 ± 0.36	1.67 ± 0.40	0.99 ± 0.18	1.96 ± 0.47	1.57 ± 0.26	1.46 ± ± 0.25	1.84 ± 0.43	1.51 ± 0.25
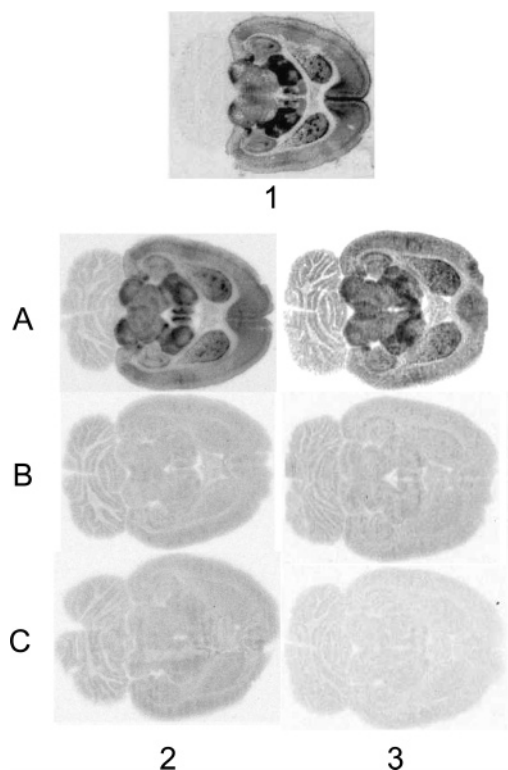
Figure 2. Autoradiography of rat brain slices incubated in vitro with no carrier added [^{3}H]DAMGO (1), [^{18}F]**4** (2), or [^{18}F]-**6** (3) under control conditions (A), in the presence 10 μM naloxone (B) or in the presence of 1.5 μM sufentanil (C).

the known distribution of μ-OR expression in rat.[24] Thalamic and striatal regions were labeled in a manner similar to that obtained with the μ-OR specific compound [^{3}H]DAMGO,[25] with relatively low labeling of nontarget regions. Qualitatively, these findings support the specificity of [^{18}F]**4** and [^{18}F]**6** for the μ-OR in brain tissue.

Molecular Modeling. Structural data on μ-ORs are limited, and several theoretical models, mostly based on the rhodopsin structure,[26] have been proposed so far.[27] These models can be extremely useful for studying antagonist−receptor interactions or for retrieving new antagonists via virtual screening from chemical databases.[28] On the other hand, evidence exists that receptor structural alterations, known to accompany the activation process,[29] have to be incorporated to properly model the agonist−receptor complex.[28] Here, to rationalize the developed SARs, the AutoDock program was used to automatically dock **6** into the μ-receptor model recently reported by Fowler et al.[15] We chose this receptor model as it provides the first presentation of the μ-OR in an active conformation. According to the X-ray structures,[30] spectroscopic data,[31] and prior computational investigations,[32] the ligand was docked with the piperidine ring in chair conformation and with both 2-thienylethyl and *N*-phenylpropanamide substituents in equatorial position.

To select a meaningful binding mode, for each solution the agreement with the experimentally known interactions for opioid agonists was taken into account . D147 [33] in TM3 is thought to bind the opioid agonists through an ionic interaction with the positively charged nitrogen.[34] For the docked compound, only two binding orientations, which located the ligand below the extracellular loops within a binding site crevice between TM3, TM5, TM6, and TM7, were found to satisfy the abovementioned condition.

In both orientations (Figure 3a,b), the protonated nitrogen forms a hydrogen bond with the carboxylate group of D147 (TM3), while the 4-axial substituent of the piperidine ring (CH$_2$OCH$_3$) interacts with the ϵ-amino group of K233 (TM5). Direct contacts between opioid ligands and D147 or K233 have been extensively documented.[34] The two docking positions substantially differ for the allocation of the ligand aromatic moieties. In a first orientation (Figure 3a), the 4-phenylpropanamide moiety inserts into the pocket made up of aromatic side chains (Y148, F152, F237, W293, and H297) and is stabilized by multiple aromatic−aromatic interactions while the thiophene ring orients toward the extracellular surface facing a shallow hydrophobic pocket formed by Y75, W318, H319, and I322 residues. A similar arrangement for a fentanyl analogue in the μ-OR has been already proposed.[35]

In the binding mode shown in Figure 3b, the thiophene ring is instead directed toward the intracellular end of the receptor binding cavity and the 4-phenylpropanamide fragment faces toward the W318 and H319 residues with its end allocating just under the EL2 sheet structures. The latter binding position is in accordance with a previously proposed binding mode of OHMe-fentanyl,[36] and with mutagenesis experiments, which together confirm the importance of H319 for the binding of OHMe-fentanyl.[37]

More recently, new experiments suggested an interaction between the 4-fluorophenylpropanamide of *p*-fluorofentanyl and H319 residue, shedding new light on the binding mode of 4-AP ligands.[38] Thus, the ligand orientation depicted in Figure 3b seems the most reasonable choice. Compared to the binding mode previously reported for OHMe-fentanyl,[36] in our **6**/μ-receptor complex model, the 4-phenylpropamamide group of the ligand is not as close to H319 as the corresponding
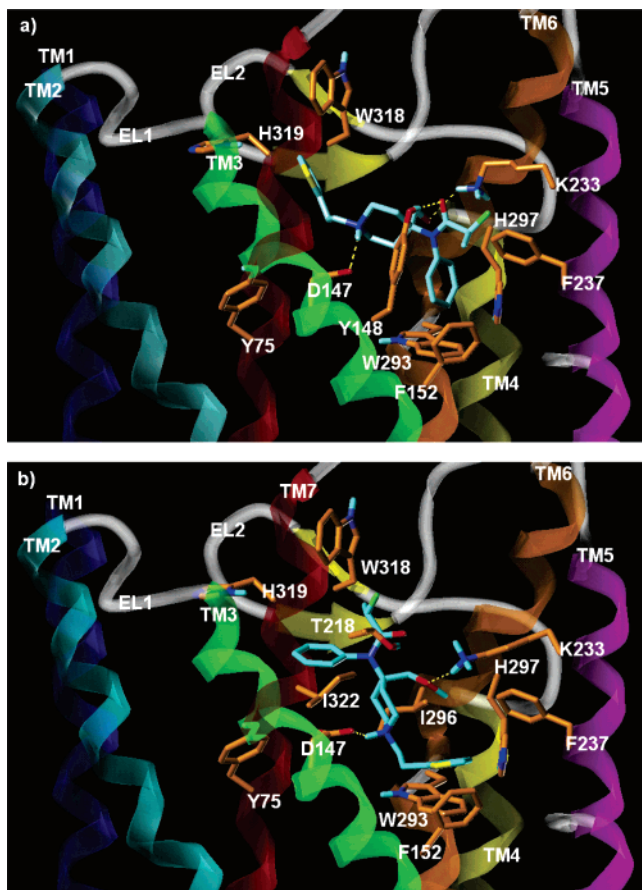
Figure 3. Two potential binding modes of **6** within the human μ-opioid receptor. The TM helices are in different colors and denoted by arabic numerals. The carbon atoms of the ligand and that of the receptor residues are displayed in cyan and orange, respectively. Hydrogen bonds are indicated by yellow dashed lines.

portion in OHMe-fentanyl and would rather establish hydrophobic interaction with I322. This is due to presence of the 4-axial substituent and its favorable interaction with K233 (TM5) and would be in accordance with the observation that sufentanil is less sensitive to H319 mutation with respect to fentanyl.[38]

The placement of aliphatic (e.g. **4**) or aromatic (e.g. **6**) groups in the pocket formed by the cluster of conserved aromatic residues, which is known to participate with the receptor activation process, would account for the agonist activity shown by our compounds.[39−40]

The proposed model correlates well with the SARs developed in the present study. The involvement of the 4-axial substituent in a hydrogen bond, with a conserved residue among the opioid receptors, accounts for the enhanced activity of carfentanil and sufentanil in all tree OR types, μ-, δ, and κ compared to that of fentanyl.[13d] Accordingly, the binding affinity of **3** is higher with respect to that of **4** (Table 1). On the basis of our model, the reduced activity of **1** compared to carfentanil can be described to the electron-withdrawing power of fluorine atom, which decreases the electron density on the oxygen atoms thereby reducing the strength of the observed hydrogen bond. The reduced affinity of **2** vs carfentanil would be due to both electronic and steric effects. The drop in activity of **2** compared to **1** is

consistent with the insertion of the 4-axial substituent in a fairly restricted region formed by K233, F237, I296, and V300.

From the results of the present study it emerges that the decrease in aromaticity, resulting from the formal N^1-5-fluoropentyl-for-N^1-phenethyl substitution, lowers the affinity from 1.1[13d] for fentanyl to 13.5 nM for **3** and from 0.02[13d] for carfentanil to 0.7 nM for **4** (Table 1). This can be explained with the loss of the favorable interactions with the cluster of aromatic side chains. Concerning **5** and **6**, both were shown to give a μ-OR affinity very close to their respective parent compounds, demonstrating that a fluorine atom in that position does not influence the binding. As already proposed by Subramanian et al.,[41] the alkyl chain next to the amide group is oriented toward the extracellular side of the binding cavity. However, in our model, the alkyl chain locates just below the EL2 residues and, due to the inaccuracy of loop structure prediction, any detailed examination of the interactions would be not meaningful.

Conclusion. The studies reported here were intended to explore the properties of a series of ¹⁸F-labeled 4-anilidopiperidines in terms of biokinetic properties, receptor affinity, and selectivity. The compounds were prepared by alterations to the lead structure as well as by variations of the labeling position. The replacement of the N^1-phenethyl moiety with a N^1-5-fluoropentyl substituent did not dramatically affect the molecular recognition and binding of the ligand in the μ-opioid receptor. The radiolabeling approaches based on *N*-phenylamine acylation were shown compatible with CH_2OMe and $COOCH_3$ substituents; thus, these functionalities are useful for a fine-tuning of pharmacokinetic and -dynamic properties of fluoro-4-AP derivatives. Key features of the ¹⁸F-labeled 4-APs governing brain uptake, stability in the brain, and brain uptake of peripherally generated radioactive metabolites have been established. Of the six compounds evaluated, [¹⁸F]-**4** ([¹⁸F]fpe-Caf) and [¹⁸F]**6** ([¹⁸F]fpr-Suf) fulfill all preclinical requirements for in vivo imaging of the μ-opioid receptor with PET. Finally, a theoretical study of the 4-AP fluorinated agonist binding has been successful in rationalizing the developed SARs. As demonstrated by this study, the combination of 3D docking studies with radiopharmaceutical screening procedures, i.e., brain uptake studies, affinity studies, autoradiography, and quantification of metabolites, provide an experimental environment for rapid development of receptor targeted radiopharmaceuticals for the CNS.

Experimental Section

General Methods. The syntheses and radiosyntheses of fluorinated esters of carfentanil **1**, **2**, [¹⁸F]**1**, and [¹⁸F]**2** from carfentanil carboxylic acid **15** (Scheme 1 and 2) were reported previously.[42] The compounds *nor*-fentanyl **16**, *des*-propionylfentanyl **17**, and *des*-propionylsufentanil **18** were obtained from Janssen Pharmaceuticals (Beerse, Belgium). The purities of **1**,**2** *nor*-fentanyl, *des*-propionylfentanyl, and *des*-propionyl sufentanil were determined by means of RP-HPLC (see below). UV-purity at 254 nM of all five compounds was determined to be >95%.

Kryptofix 2.2.2. and acetonitrile were obtained from Merck Eurolab (Darmstadt, Germany). 1-Bromo-5-fluoro pentane was obtained from Narchem Corporation, Chicago, IL. All other chemicals were purchased from Sigma-Aldrich (Taufkirchen,

Germany). All commercial reagents and solvents were used without further purification unless otherwise specified.

Column chromatography was performed on Kieselgel 60 (0.040−0.063 mm) from Merck Eurolab with *n*-hexane and ethyl acetate as eluents. Solvent composition is expressed on a volume: volume (v/v) basis. TLC was performed using Alugram Sil G/UV$_{254}$ aluminum sheets from Macherey-Nagel (Dueren, Germany) with the following eluent systems (v/v): A: *n*-hexanes−ethyl acetate 8:2; B: chloroform−methanol 9:1; C: ethyl acetate−methanol 8:2. The spots were visualized with a 254 nm UV lamp or with 5% phosphomolybdic acid in ethanol.

Apparent drug lipophilicity was determined by a conventional partition method between 1-octanol phase and phosphate-buffered saline (PBS), pH 7.4. The 1-octanol was saturated with PBS before use. Briefly, the nca ^{18}F-labeled compound in question, contained in 4 mL of PBS, was added to 4 mL of 1-octanol in a 20 mL test tube. The tube was sealed and vigorously shaken at room temperature for 10 min. The mixture was then centrifuged at 3000*g* for 10 min. A 20 μL aliquot from each of the two phases were drawn, and their radioactivity content was determined in a γ-counter. The log $P_{oct/PBS}$ was calculated as follows:

log $P_{oct/PBS}$ = log(radioactivity concentration in the 1-octanol phase/radioactivity concentration in the PBS phase). The reported values represent the mean of three independent measurements.

Analytical HPLC was performed using a Nucleosil 100 5 μm CN 4.6 × 250 mm reverse phase column (CS-Chromatographie (CS-C), Langerwehe, Germany) eluted with acetonitrile/ 0.1 M ammonium formate (55:45, v/v) mobile phase mixture and a Nucleosil 100 5 μm C18 4.6 × 250 mm reverse phase column (CS-C) eluted with acetonitrile/0.1 M ammonium formate (65:35, v/v). The flow rate was in both cases 1.0 mL/ min. The chromatography systems were fitted with a UV detector (Sykam Model S3210 set at 254 nm; Sykam, Fuerstenfeldbruck, Germany). For detection of radioactive compounds, a NaI(Tl) detector was used in series with the UV detector. Preparative HPLC was performed using a PRP-1 10 μm 10 × 50 mm sample enrichment column (CS-C) for concentration of the reaction mixture. After the concentration step, the sample enrichment column was eluted in the reverse direction onto a μ-Bondapak 5 μm 8 × 300 mm C18 column (CS-C) using a linear gradient of 15% to 70% B in 20 min (A = 0.1% TFA in water, B = 0.1% TFA in MeCN); flow rate 3 mL/min. In-line HPLC detectors included a UV detector (Sykam, set at 254 nm) and a γ-ray detector (Bioscan Flow-Count fitted with a PIN detector).

The capacity factor, *k'*, is calculated as follows:

$$k' = (t_R - t_0)/t_0$$

where t_R = retention time of the substance in question (min) and t_0 = dead volume of the column (mL)/flow (mL × min^{-1}).

Mass spectra were acquired under electron ionization (EI) conditions using a liquid chromatography mass spectroscopy system LCQ from Finnigan (Bremen, Germany) and a Hewlett-Packard series 1100 HPLC system. NMR spectra were recorded on Bruker 250 and 500 MHz spectrometers at 20 °C in CDCl$_3$ and in D$_2$O using tetramethylsilane (TMS) as an internal standard. Chemical shift (δ) values for proton resonances are reported in parts per million (ppm) relative to the internal standard TMS.

[^{18}F]Fluoride was produced through the ^{18}O(p,n)^{18}F nuclear reaction. The [^{18}F]fluoride was obtained in a 34 mM solution of K$_2$CO$_3$ (0.3 mL) and added to a 2 mL conical vial containing 0.5 mL dry MeCN and 15 mg (39.9 μmol) Kryptofix 2.2.2. The solvent was evaporated under reduced pressure at 105 °C. Azeotropic drying was repeated three times with 0.5 mL portions of MeCN prior to substitution reactions.

All animal studies were performed in accordance with the German law on the protection of animals.

Syntheses of Precursors and Standard Samples. (±)-2-Fluoropropionyl Chloride (7). The compound was prepared according to the procedure published previously.[43] ^{1}H NMR (250 MHz, CDCl$_3$) δ: 5.29 (q, 1H, J = 48 Hz); 1.73 (d, 3H, J = 23 Hz).

Syntheses of Methyl 4-[*N*-(1-Oxopropyl)-*N*-phenyl-amino]-4-piperidinecarboxylate (8; *nor*-Carfentanil). 4-Phenylamino-1-benzyl-4-piperidinecarbonitrile (10). 18.9 g (100 mmol) of *N*-benzyl-4-piperidone and 9.4 g (100 mmol) aniline were dissolved in 70 mL acetic acid. A solution of 7.2 g (110 mmol) potassium cyanide in 20 mL of water was added dropwise while keeping the temperature below 20 °C. The reaction mixture was stirred at 20 °C for 48 h. The mixture was thereafter poured into crushed ice (100 g) and basified with 130 mL of 25% ammonium hydroxide. The aqueous layer was extracted with 3 × 150 mL of chloroform. The combined organic phases were washed with 3 × 70 mL water, dried (Na$_2$-SO$_4$), and concentrated under reduced pressure. Crystallization from 60 mL of ethanol gave 17.0 g (58%) of the product. ^{1}H NMR (500 MHz, CDCl$_3$) δ: 7.14−7.27 (m, 5H, CH$_2$*Ph*); 7.15− 7.18 (m, 3H, NH*Ph*); 6.81−6.85 (m, 2H, NH*Ph*); 3.55 (s, 1H, N*H*); 3.47 (s, 2H, *CH*$_2$Ph); 2.73 (m, 2H, CH$_2$*CH*$_2$); 2.38 (m, 2H, CH$_2$*CH*$_2$); 2.25 (m, 2H, CH$_2$*CH*$_2$); 1.84 (m, 2H, CH$_2$*CH*$_2$). ^{13}C NMR (CDCl$_3$) δ: 143.37 (N*Ph*-C1); 138.08 (Bn-C1); 129.34 (N*Ph*-C3,5); 129.03 (Bn-C2,6); 128.39 (Bn-C3,5); 127.29 (Bn-C4); 120.98 (N*Ph*-C4); 120.75 (CN); 117.87 (N*Ph*-C2,6); 62.65 (Bn*CH*$_2$); 53.15 (C4); 49.34 (C2,6); 36.19 (C3,5).

4-Phenylamino-1-benzyl-4-piperidinecarboxamide (11). To 60 mL of concentrated H$_2$SO$_4$ was added 17.0 g (58.3 mmol) of **10** in portions while keeping the temperature below 5 °C. Upon completion, the mixture was allowed to warm to room temperature whereupon stirring was continued for 16 h. Thereafter, the solution was poured onto a mixture of 250 g of crushed ice and 150 mL of 25% ammonium hydroxide, and the resulting aqueous suspension was extracted with 3 × 150 mL of chloroform. The organic extract was washed with 3 × 100 mL of water. After separation of the layers, the organic phase was dried with Na$_2$SO$_4$ and concentrated in vacuo. The residue was recrystallized from 500 mL of ethanol yielding 14.07 g (77%) of **11**. ^{1}H NMR (500 MHz, CDCl$_3$) δ: 7.13−7.23 (m, 5H, CH$_2$*Ph*); 7.10 (t, 2H, NH*Ph*); 6.80 (s,1H, N*H*$_2$); 6.71 (t, 1H, NH*Ph*); 6.55 (d, 2H, NH*Ph*); 5.58 (s,1H, N*H*$_2$); 3.40 (s, 2H, *CH*$_2$Ph); 2.66 (m, 2H, CH$_2$*CH*$_2$); 2.24 (m, 2H, CH$_2$*CH*$_2$); 2.02 (m, 2H, CH$_2$*CH*$_2$); 1.84 (m, 2H, CH$_2$*CH*$_2$). ^{13}C NMR (500 MHz, CDCl$_3$) δ: 178.66 (*C*ONH$_2$); 143.74 (N*Ph*-C1); 138.28 (Bn-C1); 129.22 (N*Ph*-C3,5); 128.99 (Bn-C2,6); 128.27 (Bn-C3,5); 127.10 (Bn-C-4); 119.24 (N*Ph*-C4); 116.19 (N*Ph*-C2,6); 63.01 (Ph*CH*$_2$); 58.28 (C4); 48.76 (C2,6); 31.36 (C3,5).

4-Phenylamino-1-benzyl-4-piperidinecarboxylic Acid (12). 5.5 g (98 mmol) potassium hydroxide was dissolved in 50 mL of 1,2-ethanediol at 100 °C. The resulting solution was cooled to 70 °C, and 4-phenylamino-1-benzyl-4-piperidinecar-boxamide (**11**) (10.0 g, 32.3 mmol) was added. The reaction mixture was stirred at 190 °C for 16 h in an autoclave. The mixture was cooled and poured into 100 mL of water. The solution was filtered and neutralized with 10 mL of acetic acid. The resulting precipitate was collected and subsequently air-dried. Recrystallization form 120 mL of *N,N*-dimethylforma-mide yielded 7.76 g (76%) of the product. ^{1}H NMR (500 MHz, DMSO-d_6) δ: 7.22−7.34 (m, 5H, CH$_2$*Ph*); 7.01−7.06 (m, 2H, NH*Ph*); 6.50−6.58 (m, 3H, NH*Ph*); 3.48 (s, 2H, *CH*$_2$Ph); 2.53 (s, 1H, N*H*); 2.51 (m, 2H, CH$_2$*CH*$_2$); 2.34−2.43 (m, 2H, CH$_2$*CH*$_2$); 1.99−2.07 (m, 2H, CH$_2$*CH*$_2$); 1.91−1.98 (m, 2H, CH$_2$*CH*$_2$).

Methyl 4-Phenylamino-1-benzyl-4-piperidinecarboxy-late (13). To a suspension of 1.25 g of sodium hydride in *N,N*-dimethylformamide (40 mL) under argon was added a solution of 4-phenylamino-1-benzyl-4-piperidinecarboxylic acid (**12**) (8.83 g, 28.4 mmol) in 100 mL of *N,N*-dimethylformamide. To the suspension of the precipitated sodium salt was added methyl iodide (1.95 mL, 31.28 mmol) dropwise. The resulting mixture was stirred at room temperature for 48 h. The product mixture was poured into 170 mL of water and extracted with 3 × 150 mL of chloroform. The organic layer was washed with 100 mL of water, dried (Na$_2$SO$_4$), and evaporated in vacuo. The crude product was purified by flash-chromatography on

500 g Kieselgel using chloroform as eluent, yielding 3.9 g of **13** (42%) as a yellowish oil. ^{1}H NMR (500 MHz, CDCl$_3$) δ: 7.15−7.24 (m, 5H, CH$_2$*Ph*); 7.06 (t, 2H, NH*Ph*); 6.66 (t, 1H, NH*Ph*); 6.49 (d, 2H, NH*Ph*); 3.82 (s,1H, N*H*); 3.59 (s, 3H, COOC*H*$_3$); 3.42 (s, 2H, *CH*$_2$Ph); 2.51 (m, 2H, CH$_2$*CH*$_2$); 2.33 (m, 2H, CH$_2$*CH*$_2$); 2.16 (m, 2H, CH$_2$*CH*$_2$); 1.94 (m, 2H, CH$_2$*CH*$_2$). ^{13}C NMR (CDCl$_3$) δ: 175.95 (*C*OOCH$_3$); 144.99 (N*Ph*-C1); 138.38 (Bn-C1); 129.11 (N*Ph*-C3,5); 129.04 (Bn-C2,6); 128.24 (Bn-C3,5); 127.04 (Bn-C4); 118.56 (N*Ph*-C4); 115.29 (N*Ph*-C2,6); 62.99 (Ph*C*H$_2$); 58.27 (C-4); 52.29 (COO*C*H$_3$); 48.92 (C-2,6); 33.00 (C-3,5).

Methyl 4-[*N*-(1-Oxopropyl)-*N*-phenylamino]-1-benzyl-4-piperidinecarboxylate (14). Methyl 4-phenylamino-1-benzyl-4-piperidinecarboxylic acid (**13**) (2.44 g, 7.52 mmol) and 10 mL (76.1 mmol) of propionic anhydride were stirred and refluxed for 6 h. The resulting mixture was cooled to room temperature and diluted with 50 mL of water and was thereafter extracted with 3 × 100 mL of chloroform. The organic phases were combined, washed with 3 × 80 mL of water and once with 60 mL of saturated NaCl solution, dried (Na$_2$SO$_4$), and finally evaporated under reduced pressure. The resulting residue was dissolved in 20 mL of 2-propanol, and 0.95 g of oxalic acid in 15 mL of 2-propanol was added. A yellow crystalline precipitate formed which was filtered and dried at 3 × 10^{-1} mbar for 24 h, giving 1.6 g of **14** as the oxalate salt. A suspension of the oxalate salt in water (100 mL) was alkalized with 25% ammonium hydroxide (10 mL) followed by extraction into 300 mL of chloroform. The solvent was dried with Na$_2$SO$_4$. Concentration under reduced pressure gave 0.65 g (23%) of the title compound as a yellowish oil. ^{1}H NMR (500 MHz, CDCl$_3$) δ: 7.11−7.36 (m, 10H, CH$_2$*Ph*, N*Ph*); 3.71 (s, 3H, COOC*H*$_3$); 3.37 (s, 2H, *CH*$_2$Ph); 2.52 (m, 2H, CH$_2$*CH*$_2$); 2.31 (m, 2H, CH$_2$*CH*$_2$); 2.18 (m, 2H, CH$_2$*CH*$_2$); 1.85 (q, *J* = 7.4 Hz, 2H, *CH*$_2$CH$_3$); 1.55 (m, 2H, CH$_2$*CH*$_2$); 0.87 (t, *J* = 7.4 Hz, CH$_2$*CH*$_3$).

Methyl 4-[*N*-(1-Oxopropyl)-*N*-phenylamino]-4-piperidinecarboxylate (8). A solution of methyl 4-[*N*-(1-oxopropyl)-*N*-phenylamino]-1-benzyl-4-piperidinecarboxylate (**14**) (0.65 g, 1.7 mmol) in ethanol (50 mL) was hydrogenated in the presence of 10% Pd/C (200 mg) at atmospheric pressure and room temperature. After 24 h the catalyst was removed by filtration and the filtrate was concentrated. The residue was purified by column chromatography (60 g Kieselgel; eluent [B]), yielding 0.26 g of the product (52%) which was dried at 3 × 10^{-1} mbar for 16 h. Analytical HPLC: reverse phase CN (55/45 acetonitrile/0.1 M ammonium formate), *k'* = 1.4, purity 98.8%; reverse phase C18 (65/35 acetonitrile/0.1 M ammonium formate), *k'* = 1.7, purity 98.5%; ^{1}H NMR (500 MHz, CDCl$_3$) δ: 8.07 (s,1H, N*H*); 7.29−7.45 (m, 5H, N*Ph*); 3.80 (s, 3H, COOC*H*$_3$); 3.14−3.19 (m, 4H, CH$_2$*CH*$_2$); 2.35−2.40 (m, 2H, CH$_2$*CH*$_2$); 1.87−1.94 (m, 2H, CH$_2$*CH*$_2$); 1.86 (q, *J* = 7.4 Hz, 2H, *CH*$_2$CH$_3$); 0.94 (t, *J* = 7.4 Hz, 3H, CH$_2$*CH*$_3$). ^{13}C NMR (CDCl$_3$) δ: 174.43 (*C*OOCH$_3$); 172.99 (CH$_3$*C*H$_2$*C*O); 138.48 (N*Ph*-C1); 130.40 (N*Ph*-C2,6); 129.74 (N*Ph*-C3,5); 129.25 (N*Ph*-C4); 61.04 (C4); 52.70 (COO*C*H$_3$); 41.16 (C-2,6); 30.65 (C-3,5); 28.95 (CH$_3$*C*H$_2$CO); 9.11 (*C*H$_3$CH$_2$CO).

2-Bromopropionic Acid 9′-Anthryl Methyl Ester (9). The compound was prepared according to a previously published procedure.[44] ^{1}H NMR (250 MHz, CDCl$_3$) δ: 7.28−8.51 (m, 9H); 6.18 (s, 2H,) 4.39 (q, 1H, *J* = 7.0 Hz); 1.78 (d, 3H, *J* = 7.0 Hz).

N-[1-(5-Fluoropentyl)-4-piperidinyl]-N-phenylpropan-amide (3). To a solution of *nor*-fentanyl (80 mg, 0.34 mmol) in 7 mL of anhydrous tetrahydrofuran was added dried potassium carbonate (50 mg, 0.36 mmol), and the mixture was stirred at room temperature for 20 min. Thereafter, 5-fluoropentyl bromide (64 mg, 0.38 mmol) was added, and the mixture was heated at reflux under argon for 5 h. After cooling, the mixture was concentrated under reduced pressure. Twenty milliliters of dichloromethane was added to the residue and partitioned with water (20 mL). The water phase was washed with 20 mL of dichloromethane, and the combined organic extracts were dried (MgSO$_4$), filtered, and concentrated to an oil which was purified by RP-HPLC (Luna C$_{18}$ 5 μm, 10 mm ×

250 mm; Phenomenex, Torrence, CA) using a linear gradient of 15% to 70% B in 20 min; 0.1% TFA in water (A), 0.1% TFA in MeCN (B), flow rate of 3 mL/min. The eluent was continuously monitored for UV absorbance (254 nm). The fraction containing the product (capacity factor, *k'* = 7.4) was evaporated to yield 49.6 mg of a colorless oil (45.6%). ^{1}H NMR (250 MHz, CDCl$_3$) δ: 7.18−7.32 (m, 5H, N*Ph*), 3.52 (m, 1H, CH$_2$*CH*); 3.96 (d, 2H, *J* = 42.1 Hz, F*CH*$_2$); 3.08−3.28 (q, 2H, FCH$_2$CH$_2$-CHCH$_2$*CH*$_2$N); 2.57−2.66 (m, 2H, CH$_2$*CH*$_2$); 2.48−2.54 (m, 2H, CH$_2$*CH*$_2$); 2.11−2.18 (m, 2H, CH$_2$*CH*$_2$); 1.98−2.04 (m, 2H, CH$_2$*CH*$_2$); 1.63 (q, 2H, *J* = 7.4 Hz, *CH*$_2$CH$_3$); 1.54−1.62 (m, 2H, FCH$_2$*CH*$_2$); 1.43−1.50 (m, 2H, FCH$_2$CH$_2$CH$_2$*CH*$_2$); 1.28−1.36 (m, 2H, FCH$_2$CH$_2$*CH*$_2$CH$_2$); 0.92 (t, 3H, *J* = 7.4 Hz, CH$_2$*CH*$_3$). ^{13}C NMR (250 MHz, CDCl$_3$) δ: 172.85 (*C*OCH$_2$CH3); 141.55 (N*Ph*-C1); 135.43 (N*Ph*-C2,6); 129.64 (N*Ph*-C3,5); 128.31 (N*Ph*-C4); 85.08 (F*C*H$_2$CH$_2$CH$_2$CH$_2$CH$_2$); 55.31 F*C*H$_2$-CH$_2$CH$_2$CH$_2$CH$_2$; 50.49 (C2,6); 49.24 (C4); 33.14 (FCH$_2$*C*H$_2$-CH$_2$CH$_2$CH$_2$); 34.22 (C3,5); 30.76 (FCH$_2$CH$_2$*C*H$_2$CH$_2$CH$_2$); 24.11 (FCH$_2$CH$_2$CH$_2$*C*H$_2$CH$_2$); 29.14 (CO*C*H$_2$CH$_3$); 9.23 (COCH$_2$-*C*H$_3$). MS calcd for C$_{19}$H$_{29}$FN$_2$O = 320.2; found, 321.2 [M + H]$^+$.

Methyl 4-[*N*-(1-Oxopropyl)-*N*-phenylamino]-1-(5-fluoropentyl)-4-piperidinecarboxylate (4). Compound **4** was prepared from **8** (58 mg, 0.2 mmol) using the procedure for **3**. The fraction from the preparative HPLC with *k'* = 7.9 was collected and concentrated under reduced pressure yielding a yellowish oil (38.8 mg, 51.3%). ^{1}H NMR (250 MHz, CDCl$_3$) δ: 7.31−7.47 (m, 5H, NH*Ph*); 3.94 (d, 2H, *J* = 42.1 Hz, F*CH*$_2$); 3.82 (s, 3H, COOC*H*$_3$); 3.04−3.22 (q, 2H, FCH$_2$CH$_2$CHCH$_2$-*CH*$_2$N); 2.48−2.56 (m, 2H, CH$_2$*CH*$_2$); 2.26−2.34 (m, 2H, CH$_2$*CH*$_2$); 2.14−2.21 (m, 2H, CH$_2$*CH*$_2$); 1.83 (q, 2H, *J* = 7.4 Hz, *CH*$_2$CH$_3$); 1.52−1.57 (m, 2H, CH$_2$*CH*$_2$); 1.56−1.62 (m, 2H, FCH$_2$*CH*$_2$); 1.43−1.50 (m, 2H, FCH$_2$CH$_2$CH$_2$*CH*$_2$); 1.30−1.38 (m, 2H, FCH$_2$CH$_2$*CH*$_2$CH$_2$); 0.91 (t, 3H, *J* = 7.4 Hz, CH$_2$*CH*$_3$). ^{13}C NMR (250 MHz, CDCl$_3$) δ: 176.85 (*C*OCHFCH$_3$); 174.73(*C*OOCH$_3$); 145.43 (NPh-C1); 133.43 (NPh-C2,6); 129.64 (NPh-C3,5); 128.31 (NPh-C4); 92.96 (CO*C*HFCH$_3$); 85.17 (F*C*H$_2$CH$_2$CH$_2$CH$_2$CH$_2$); 58.54 (C4); 56.78 F*C*H$_2$CH$_2$CH$_2$-CH$_2$CH$_2$; 52.23 (COO*C*H$_3$); 48.69 (C2,6); 33.46 (FCH$_2$*C*H$_2$CH$_2$-CH$_2$CH$_2$); 32.82 (C3,5); 31.10 (FCH$_2$CH$_2$CH$_2$*C*H$_2$CH$_2$); 24.92 (FCH$_2$CH$_2$*C*H$_2$CH$_2$CH$_2$); 17.87 (COCHF*C*H$_3$). MS calcd for C$_{21}$H$_{31}$FN$_2$O$_3$ = 378.2; found, 379.2 [M + H]$^+$.

(±)-*N*-Phenyl-*N*-[1-(2-phenylethyl)-4-piperidinyl]-2-fluoropropanamide (5). To a solution of *des*-propionylfentanyl (112 mg, 0.40 mmol) in tetrahydrofuran (6 mL), triethylamine (61.2 μL, 0.44 mmol) was added. To the mixture (±)2-fluoropropionyl chloride (**7**) (52.8 mg, 0.48 mmol), dissolved in 4 mL of tetrahydrofuran, was added dropwise at room temperature. The mixture was heated at reflux for 1 h and thereafter concentrated under reduced pressure. The residue was dissolved in dichloromethane (30 mL) and partitioned with water (30 mL). The aqueous phase was washed once with 30 mL of dichloromethane. The combined organic phases were dried (MgSO$_4$), filtered and concentrated to an oil which was purified by reverse-phase HPLC as described for **3**. The fraction containing the product (*k'* = 8.9) was evaporated to yield 35.2 mg of a colorless oil (24.8%). ^{1}H NMR (250 MHz, CDCl$_3$) δ: 7.12−7.34 (m, 7H, CH$_2$CH$_2$*Ph*, N*Ph*); 6.64 (t, 1H, N*Ph*); 6.60 (d, 2H, N*Ph*); 4.54−4.45 (m, 1H, *J* = 46.4 Hz, *CH*FCH$_3$); 3.60 (m, 1H, CH$_2$*CH*); 3.20−3.55 (m, 2H, *CH*$_2$CH$_2$-Ph) 2.90−2.98 (m, 2H, CH$_2$*CH*$_2$Ph); 2.78−2.85 (m, 2H, CH$_2$*CH*$_2$); 2.58−2.64 (m, 2H, CH$_2$*CH*$_2$); 2.18−2.26 (m, 2H, CH$_2$*CH*$_2$); 2.06−2.14 (m, 2H, CH$_2$*CH*$_2$); 1.22−1.30 (m, 3H, *J* = 22.3 Hz, CH$_2$*CH*$_3$). ^{13}C NMR (CDCl$_3$) δ: 176.78 (*C*OCH$_2$CH$_3$); 92.36 (CO*C*HFCH$_3$); 142.86 (N*Ph*-C1); 140.25 (N*Ph*-C2,6) 139.78 (Ph-C1) (129.42, N*Ph*-C3,5); 128.76 (Ph-C2,C6); 127.45 (Ph-C3,5); 126.21 (N*Ph*-C4); 124.42 (Ph-C4); 60.67 (C4) 52.44 (Ph*C*H$_2$*C*H$_2$); 49.94 (C2,6); 34.48 (Ph*C*H$_2$CH$_2$); 32.63 (C3,C5); 17.82 (COCHF*C*H$_3$). MS calcd for C$_{22}$H$_{27}$FN$_2$O = 354.2; found, 355.2 [M + H]$^+$.

(±)-*N*-Phenyl-*N*-[4-(methoxymethyl)-1-[2-(2-thienyl)-ethyl]-4-piperidinyl]-2-fluoropropanamide (6). The desired product **6** was obtained from *des*-propionylsufentanil (66 mg, 0.20 mmol) using the procedure for **5**. The fraction from

the preparative HPLC with $k' = 9.2$ was collected and concentrated under reduced pressure yielding a yellowish oil (25.8 mg, 31.8%). ^{1}H NMR (250 MHz, CDCl$_3$) δ: 7.12−7.18 (m, 2H, N*Ph*); 7.04 (m, 1H, thiophene); 6.88−6.94 (m, 2H, *t*hiophene); 6.85 (t, 1H, N*Ph*); 6.77−6.82 (m, 2H, N*Ph*); 4.51−4.58 (m, 1H, $J = 46.2$ Hz, CO*CH*FCH$_3$); 3.36 (s, 2H, *CH$_2$*-COC*H$_3$*); 3.32 (s, 3H, CH$_2$COC*H$_3$*); 3.01−3.08 (m, 2H, CH$_2$*CH$_2$*); 2.62−2.74 (m, 4H, thiophene-*CH$_2$CH$_2$*); 2.50−2.58 (m, 2H, CH$_2$*CH$_2$*); 1.94−2.00 (m, 2H, CH$_2$*CH$_2$*); 1.75−1.82 (m, 2H, CH$_2$*CH$_2$*); 1.20−1.28 (m, 3H, $J = 22.3$ Hz, COCHF*CH$_3$*). ^{13}C NMR (250 MHz, CDCl$_3$) δ: 176.65 (*C*OCHFCH$_3$); 146.43 (N*Ph*-C1); 141.61 (thiophene-C1); 133.43 (N*Ph*-C2,6); 130.64 (N*Ph*-C3,5); 129.31 (N*Ph*-C4); 125.43 (thiophene-C3); 123.74 (thiophene-C2); 122.15 (thiophene-C4); 92.76 (CO*C*HFCH$_3$); 75.95 (*C*H$_2$COCH$_3$); 58.86 (thiophene-*C*H$_2$CH$_2$); 57.86 (C4); 53.91(*C*H$_2$-COCH$_3$); 47.79(C2,C6); 31.91(C3,C5); 26.87 (thiophene-*C*H$_2$-CH$_2$); 17.62 (COCHF*C*H$_3$). MS calcd for C$_{22}$H$_{29}$FN$_2$O$_2$S = 404.2; found 405.2 [M + H]$^+$.

Radiosyntheses of ^{18}F-Labeled 4-Anilidopiperidines. *N*-[1-(5-[^{18}F]Fluoropentyl)-4-piperidinyl]-*N*-phenylpropanamide ([^{18}F]3). A solution of 1,5-dibromopentane (7 mg, 30 μmol) in MeCN (250 μL) was added to the dried kryptate (K $\subset$ [2.2.2]$^+$ ^{18}F$^-$) and the vial was then sealed and heated at 90 °C for 8 min. 5-[^{18}F]Fluoropentyl bromide was purified by reversed phase HPLC (Lichrosorb 5 RP-18 10 mm × 250 mm (CS-Chromatographie-Service) eluted with MeOH/H$_2$O [60:40, v/v], 4 mL/min, $k' = 7.7$; preparative radiochemical yield 65 ± 5%). After on-line fixation of the product on a Strata X cartridge (33 μm; 30 mg/1 mL; Phenomenex, Torrance) and drying of the product by argon-flush, the product was eluted with 0.2 mL of DMF into a 2 mL reaction vial containing *nor*-fentanyl (2.0 mg, 8.6 μmol) and sodium iodide (2 mg, 13.3 μmol). The reaction mixture was heated at 120 °C for 10 min. After cooling, the reaction mixture was diluted with 4 mL of 0.1 M ammonium formate, loaded into a 7 mL injection loop, and transferred onto the sample enrichment column which was washed with water at a flow-rate of 2 mL/min for 5 min and subsequently eluted in the reverse direction onto the semi-preparative column. For animal experiments, the fraction containing the product was collected in a rotary evaporation flask containing 1 mL of 1% HCl in EtOH and evaporated to dryness under reduced pressure. The product was dissolved in 1−5 mL of isotonic saline and transferred into a vial containing 0.1 mL of an 8.4% sodium bicarbonate solution. The pH of the final solution was between 7 and 8. Radiochemical and chemical purities were >95% as determined by analytical HPLC ($k' = 3.2$ using the CN analytical column eluted with 55/45 acetonitrile/0.1 M ammonium formate). The radiochemical yield averaged 54% at end-of-syntheses (EOS) based on [^{18}F]fluoride and the specific activity averaged 76.4 GBq/μmol at EOS.

Methyl 4-(*N*-1-Oxopropyl)-*N*-phenylamino]-1-(5-[^{18}F]-fluoropentyl)-4-piperidinecarboxylate ([^{18}F]4). The radiosyntheses of [^{18}F]3 was accomplished according to the procedure for [^{18}F]3 described above. Radiochemical and chemical purities were >95% as determined by analytical HPLC ($k' = 3.3$ using the CN analytical column eluted with 55/45 acetonitrile/0.1 M ammonium formate) The radiochemical yield averaged 57% at EOS based on [^{18}F]fluoride and the specific activity averaged 67.6 GBq/μmol at EOS.

N-[1-[2-(Phenylethyl)-4-piperidinyl]-*N*-phenyl-2-[(±)-[^{18}F]fluoropropanamide] ([^{18}F]5). No carrier added (n.c.a) (±)-2-[^{18}F]fluoropropionic acid was obtained by hydrolysis of 9′-anthrylmethyl-(±)-2-[^{18}F]fluoropropionate with tetramethyl-ammonium hydroxide in aqueous methanol according to the procedure reported previously.^{44} Subsequently, a dried residue of the tetramethylammonium salt of (±)-2-[^{18}F]fluoropropionic acid was obtained by azeotropic distillation with MeCN (4 × 1 mL) at 90 °C under a steam of argon. After this the vial was sealed and phthaloyl dichloride (200 μL, 1.33 mmol) in anhydrous tetrahydrofuran (200 μL) was added, and the mixture was heated at reflux for 5 min. The heating source was removed and the vial left to cool for 2 min. Thereafter, the vial was vented via capillary PEEK tubing to a second vial

containing *des*-propionylfentanyl (4 mg, 14.3 μmol) dissolved in tetrahydrofuran (0.15 mL), kept at 0 °C. The (±)-2-[^{18}F]-fluoropropionic chloride was distilled at 90 °C at an argon gas flow rate of 20 mL/min. After 5 min, vessel B was closed and heated at 70 °C in order to promote amide formation. The solvent was removed by evaporation, and the resulting residue was dissolved in MeCN (300 μL). The product was purified, concentrated, and formulated for injection as described above for [^{18}F]3. Radiochemical and chemical purities were >95% as determined by analytical HPLC ($k' = 3.7$ using the CN analytical column eluted with 55/45 acetonitrile/0.1 M ammonium formate). The radiochemical yield averaged 36% at EOS based on [^{18}F]fluoride and the specific activity averaged 42.2 GBq/μmol at EOS.

N-[1-[2-(2-Thienyl)ethyl]-4-piperidinyl]-*N*-phenyl-2-[(±)-[^{18}F]fluoropropanamide] ([^{18}F]6); [^{18}F]fpr-Suf. The radiosyntheses of [^{18}F]6 was accomplished in a manner identical to [^{18}F]5 given above, using 4.7 mg (14.3 μmol) of precursor *des*-propionylsufentanil for the ^{18}F-fluoropropionylation. Radiochemical and chemical purities were >95% as determined by analytical HPLC ($k' = 3.9$ using the CN analytical column eluted with acetonitrile/0.1 M ammonium formate; 55/45). The radiochemical yield averaged 32% at EOS based on [^{18}F]-fluoride and the specific activity averaged 40.2 GBq/μmol at EOS.

Biodistribution in Mice. Studies were performed in male Balb-C mice (body weight of 19−25 g). The mice were injected in a lateral tail vein with 2−5 MBq of a high specific activity (>37 GBq/μmol) ^{18}F-Labeled 4-anilidopiperidine derivative contained in <0.15 mL of a solution of isotonic saline. Groups of mice were sacrificed at 5−60 min postinjection. The radioactivity of weighed tissue samples was measured in a γ-counter. Data are expressed as percent of the injected dose per gram tissue (% ID/g) (mean ± SD, $n = 3$−4).

Metabolite Analysis. Male Balb-C mice were injected with 9−17 MBq of the ^{18}F-labeled compound of study. 5−40 min after injection the animals were sacrificed and the tissue of interest was dissected. The procedure used for the analysis of plasma metabolites was as follows: Whole blood (0.2−0.4 mL) containing about 30 μL of heparin was centrifuged at 6000g for 5 min, and approximately 0.1−0.2 mL of the supernatant plasma was removed. An equal volume of acetonitrile was added, and the mixture was vortexed for 1 min and centrifuged at 6000g for 3 min. To calculate the radioactivity balance and extraction efficiency, the radioactivity from the combined liquids was compared to the radioactivity of the extracted material by γ-counter measurements (extraction efficiency >95%). Approximately 0.1 mL of the supernatant solution was analyzed using radio-HPLC [Nucleosphere 100, 5 μm; 10 × 150 mm (CS-Chromatographie); MeOH/0.1 M ammonium formate 60:40 (v/v)]. The outlet of the column was connected in-line with a solid-phase scintillation counter (Flow-one Beta, Bioscan, Washington DC).

The amount of intact tracer (T_i) was calculated as follows:

$$T_i = [F_T/F_T + F_M] \times E_E \times E_R \times 1 \times 10^{-2}$$

where F_T [%] represents the amount of intact tracer and F_M [%] the amount of metabolites as determined by radio-HPLC, corrected for extraction efficiency E_E [%] from the plasma samples and the recovery E_R [%] of activity from the HPLC.

For analysis of brain radioactivity metabolites, brain tissue homogenates were prepared immediately after dissection by mechanical homogenization of nitrogen-frozen samples followed by addition of 1 mL of phosphate-buffered saline. The mixture was vigorously vortexed, and 1 mL of MeCN was added. After centrifugation for 5 min at 6000g, the supernatant was collected. The mixture was analyzed by HPLC as described above. The percentage of intact tracer in brain (T_i) was calculated using the equation given above for the analysis of the radioactivity in plasma, and in this case the term E_E represents the efficiency of the extraction of activity from brain homogenates, (>91%).

Autoradiography. Fresh-frozen pieces of adjacent rat brain sections were used for the autoradiographic binding studies. Unfixed frozen sections (60 μm) were thawed, dried, and subsequently preincubated in 15 mM Tris-HCl buffer (pH 7.4) for 30 min followed by incubation with the ^{18}F-ligand in question (17 kBq/mL) for 1 h at ambient temperature in an aqueous 50 mM Tris-HCl buffer (pH 7.4) without or in the presence of either 10 μM naloxon (for blocking of μ, δ, and κ) or 1.5 μM sufentanil (for blocking of μ). The sections were thereafter washed twice in 50 mM Tris-HCl for 3 min and then in water for 3 min. Finally the slices were dried under an air stream at 37 °C for 8−10 min, before being exposed to autoradiography film (Kodak Biomax MR, Biostep GMBH, Jansdorf, Germany) for 6 h.

In Vitro Binding Assays with Human μ-Opioid Receptor Membranes. Human recombinant μ-opioid receptor (Euroscreen, Gosselies, Belgium) was used for determination of inhibition constants (K_i). Binding experiments were done using a membrane concentration of 1 mg/mL in a binding buffer consisting of 99.5% aqueous 50 mM Tris-HCl, 5 mM $MgCl_2$, and 0.5% EtOH, pH 7.4. The membranes were incubated with the μ-selective radioligand [3H]DAMGO[25] (2 nM) in the presence of increasing concentrations of the test compound. Reactions were terminated by rapid filtration through Whatman GF/B glass fiber filters (Whatman, Maidstone, Kent, U.K.) which in advance had been treated with 0.5% bovine serum albumin in 50 mM Tris-HCl, 5 mM $MgCl_2$, pH 7.4, followed by three washings with 5 mL of ice-cold buffer (50 mM Tris-HCl, 5 mM $MgCl_2$, pH 7.4). The bound radioactivity was measured in scintillation cocktail, using a Beckman LS1701 liquid scintillation counter (Beckman Coulter Inc., Fullerton, CA). Nonspecific binding was defined in the presence of 10 μM unlabeled carfentanil. For determination of the IC_{50} values, data were fitted with a weighted two-parameter logistic function using SigmaPlot SPSS Inc., Chicago, IL). The IC_{50} values obtained were used for calculating K_i values by using the formula: $K_i = IC_{50}/(1 + L/K_D)$ where L equals the concentration of DAMGO and K_D its dissociation constant (0.57 nM[25]). The K_i values presented for the ligands of study are the mean of three independent experiments.

Molecular Modeling. Docking Simulations. Docking of **6** within the human μ-OR was carried out using the AutoDock program package version 3.0.5.[45] The LGA algorithm, as implemented in the AutoDock program, was used applying a protocol with a maximum number of 1.5×10^{-6} energy evaluations, a mutation rate of 0.01, a crossover rate of 0.80, and an elitism value of 1. For the local search, the pseudo-Solis and Wets algorithm was applied using a maximum of 300 interactions per local search. Fifty independent docking runs were carried out. Results differing by less than 1.5 Å in positional root-mean-square deviation (rmsd) were clustered together and represented by the result with the most favorable free energy of binding. The obtained complex were energetically minimized using 3000 steps of steepest descent algorithm, permitting only the ligand and the side chain atoms of the protein within a radius of 5 Å around the ligand to relax. The geometry optimization was carried out employing the SYBYL program version 8.0 with the TRIPOS force field.[46]

Ligand Setup. Compound **6** was built from the closely related X-ray structure of fentanyl (Cambridge Structural Database, code: PEPCIT10) and was appropriately modified using the standard fragment library of the SYBYL software. **6** was modeled in its *N*-protonated form as this form is considered to be the pharmacologically relevant species. According to the X-ray structure of fentanyl, the piperidine ring of the ligand was in the chair conformation, while the 2-thienylethyl and the *N*-phenylalkylamide substituent were in equatorial position. Geometry optimizations were achieved with the SYBYL/MAXIMIN2 minimizer by applying the BFGS algorithm[47] with a convergence criterion of 0.001 kcal/mol and employing the TRIPOS force field. Partial atomic charges were assigned using Gasteiger and Marsili formalism as implemented in the SYBYL package.[48] The piperidine ring was held fixed in the chair conformation, while flexible torsions in the

1,4-diequatorial substituents and in 4-axial substituent have been taken into account during the docking simulation.

Receptor Setup. Compound **6** was docked in the model of rat μ-OR developed by Fowler et al.[15] The receptor was mutated from rat to human changing the nonconserved residues accordingly. The resulting receptor structure was energy-minimized using 3000 steps of Steepest Descent algorithms to allow the mutated residue to adjust with respect to the environment. Finally, the receptor was set up for docking as follows: the unpolar hydrogens were removed, and Kollman united-atom partial charges were assigned. Solvation parameters were added to the receptor using the ADDSOL utility of the AutoDock program. The grid maps were calculated with AutoGrid. The grids were chosen to be large enough to include a significant part of the receptor around the D147 residue though to be a primary anchor point for the ligand binding. Grid maps with $61 \times 61 \times 61$ points with a grid-point spacing of 0.375 Å were used. The center of the grid was set to be coincident with the D147 C_α.

Supporting Information Available: Experimental HPLC data for determining purity of compounds **1−6**. This material is available free of charge via the Internet at http://pubs.acs.org.

References

(1) Matthes, H. W.; Maldonado, R.; Simonin, F.; Valverde, O.; Slowe, S.; Kitchen, I.; Befort, K.; Dierich, A.; Le Meur, M.; Dolle, P.; Tzavara, E.; Hanoune, J.; Roques, B. P.; Kieffer, B. L. Loss of morphine-induced analgesia, reward effect and withdrawal symptoms in mice lacking the mu-opioid-receptor gene. *Nature* **1996**, *383*, 819−823.

(2) Rubinstein, M.; Mogil, J. S.; Japon, M.; Chan, E. C.; Allen, R. G.; Low, M. J. Absence of opioid stress-induced analgesia in mice lacking beta-endorphin by site-directed mutagenesis. *Proc. Natl. Acad. Sci. U.S.A.* **1996**, *93*, 3995−4000.

(3) Zubieta, J. K.; Smith, Y. R.; Bueller, J. A.; Xu, Y.; Kilbourn, M. R.; Jewett, D. M.; Meyer, C. R.; Koeppe, R. A.; Stohler, C. S. Regional mu-opioid receptor regulation of sensory and affective dimensions of pain. *Science* **2001**, *293*, 311−315.

(4) Bencherif, B.; Fuchs, P. N.; Sheth, R.; Dannals, R. F.; Campbell, J. N.; Frost, J. J. Pain activation of human supraspinal opioid pathways as demonstated by [11C]carfentanil and positron emission tomographpy (PET). *Pain* **2002**, *99*, 589−598.

(5) Zubieta, J. K.; Gorelick, D. A.; Stauffer, R.; Ravert, H. T.; Dannals, R. F.; Frost, J. J. Increased mu opioid receptor binding detected by PET in cocaine dependent men is associated with cocaine craving. *Nature Med.* **1996**, *2*, 1225−1229.

(6) Bencherif, B.; Wand, G. S.; McCaul, M. E.; Kim, Y. K.; Ilgin, N.; Dannals, R. F.; Frost, J. J. Mu-opioid receptor binding measured by [11C]carfentanil positron emission tomography is related to craving and mood in alcohol dependence. *Biol. Psych.* **2004**, *55*, 255−262.

(7) Liberzon, I.; Zubieta, J. K.; Fig, L. M.; Phan, K. L.; Koeppe, R. A.; Taylor S. F. μ-Opioid receptors and limbic responses to aversive emotional stimuli. *Proc. Natl. Acad. Sci. U.S.A.* **2002**, *99*, 7084−7089.

(8) Halldin, C.; Gulyás, B.; Langer, O.; Farde, L. Brain radioligands-State of the art and new trends. *Q. J. Nucl. Med.* **2001**, *45*, 139−152.

(9) Hartvig, P.; Bergström, M.; Langstöm, B. Use of positron emission tomography in analyzing receptor function in vivo. *Toxicol. Lett.* **2001**, *120*, 243−251.

(10) Laruelle, M. Imaging synaptic neurotransmission with in vivo binding competition techniques: a critical review. *J. Cereb. Blood Flow Metab.* **2000**, *20*, 423−451.

(11) Laruelle, M.; Huang, Y. Vulnerability of Positron Emission Tomography radiotracers to endogenous competition. *Q. J. Nucl. Med.* **2001**, *45*, 124−138.

(12) (a) Helsley, G. C.; Lunsford, C. D.; Welstead, W. J., Jr.; Boswell, R. F.; Funderburk, W. H.; Johnson, D. N. Synthesis and analgesic activity of aome 1-substituted 3-pyrrolidinylanilides and dihydrobenzoxazinones. *J. Med. Chem.* **1969**, *12*, 583−586. (b) Finney, Z. G.; Riley, T. N. 4-anilidopiperidine analgesics. 3.

1-substituted 4-(propananilido) perhydroazepines as ring- expanded analogues. *J. Med. Chem.* **1980**, *23*, 895–899. (c) Borne, R. F.; Law, S.-Y.; Kapeghian, J. C.; Masten, L. W. Evaluation of 2-azabicyclo[2.2.2] octane analogues of 4-anilidopiperidine analgesics. *J. Pharm. Sci.* **1980**, *69*, 1104–1106. (d) Fernandez, M. J.; Huertas, R. M.; Galvez, E.; Orjales, A.; Berisa, A.; Labeaga, L.; Gago, F.; Fonseca, I.; Sanz- Aparicio, J.; Cano, F. H.; Albert, A.; Fayor, J. Synthesis, conformational and structural, conformational and pharmaclgical studies of new fentanyl derivatives of the nor-granatane System. *J. Chem. Soc., Perkin Trans. 2* **1992**, 687–695. (e) Van Daele, P. G.; De Bruyn, M. F.; Boey, J. M.; Sanczuk, S.; Agten, J. T.; Janssen, P. A. Synthetic analgesics: *N*-(1-[2-arylethyl]-4-substituted 4-piperidinyl *N*-arylalkanamides. *Arzneim.-Forsch. Drug Res.* **1976**, *26*, 1521–1531.

(13) (a) Colapet, J. A.; Diamantidis, G.; Spencer, H. K.; Spaulding, T. C.; Rudo, F. G. Synthesis and pharmacological evaluation of 4,4-disubstituted piperidines. *J. Med. Chem.* **1989**, *32*, 968–974. (b) France, C. P.; Winger, G.; Madzihradsky, F.; Seggel, M. G.; Rice, K. C.; Woods, J. H. Mirfentanil: Pharmacological profile of a novel fentanyl derivative with opioid and nonopioid effects. *J. Pharmacol. Exp. Ther.* **1991**, *258*, 502–510. (c) France, C. P.; Gerak, L. R.; Flynn, D.; Winger, G. D.; Medzihradsky, F.; Bagley, J. R.; Brockunier, L. L.; Woods, J. H. Behavioral effects and receptor binding affinities of fentanyl derivatives in rhesus monkeys. *J. Pharmacol. Exp. Ther.* **1995**, *274*, 17–28. (d) Cometta-Morini, C.; Maguire, P. A.; Loew, G. H. Molecular determinants of μ-receptor recognition for the fentanyl class of compounds. *Mol. Pharmacol.* **1992**, *41*, 185–196.

(14) (a) Janssen, P. A. J.; Van Daele, G. H. P. *N*-(4-piperidinyl)-*N*-phenylamides and -carbamates. US patent 3,998,834, 1976. (b) Janssen, P. A. J.; Van Daele, G. H. P. *N*-(4-piperidinyl)-*N*-phenylamides. US patent 4,179,569, 1979.

(15) Fowler, C. B.; Pogozheva, I. D.; Lomize, A. L.; LeVine, H. 3rd; Mosberg, H. I. Complex of an active mu-opioid receptor with a cyclic peptide agonist modeled from experimental constraints. *Biochemistry.* **2004**, *43*, 15796–15810. The model of the μ-receptor is available from the following web site: http://mosberglab.phar.umich.edu/resources/index.php.

(16) Jewett, D. M.; Kilbourn, M. R. In vivo evaluation of new carfentanil-based radioligands for the mu opiate receptor. *Nucl. Med. Biol.* **2004**, *31*, 321–325.

(17) Saji, H.; Tsutsumi, D.; Magata, Y.; Iida, Y.; Konishi, J.; Yokoyama, A. Preparation and biodistribution in mice of [¹¹C]carfentanil: a radiopharmaceutical for studying brain μ-opioid receptors by positron emission tomography. *Ann. Nucl. Med.* **1992**, *6*, 63–67.

(18) Wester, H.-J.; Willoch, F.; Tölle, T. R.; Munz, F.; Herz, M.; Øye, I.; Schadrack, J.; Schwaiger, M.; Bartenstein, P. 6-*O*-(2-[¹⁸F]-fluoroethyl)6-*O*-desmethyl-diprenorphine ([¹⁸F]DPN): Synthesis, biological evaluation, and comparison with [¹¹C]DPN in humans. *J. Nucl. Med.* **2000**, *41*, 1279–1286.

(19) Endres, C. J.; Bencherif, B.; Hilton, J.; Madar, I.; Frost, J. J. Quantification of brain mu-opioid receptors with [¹¹C]carfentanil: reference-tissue methods. *Nucl. Med. Biol.* **2003**, *30*, 177–186.

(20) Halldin, C.; Swahn, C. G.; Farde, L.; Sedvall, G. Radioligand disposition and metabolism-Key information in drug development. In *PET for Drug Development and Evaluation*; Comar, D., Ed.; Kluwer Academic Publishers: Boston, 1995; pp 55–61.

(21) Carson, R. E.; Lang, L.; Watabe, H.; Der, M. G.; Adams, H. R.; Jagoda, E.; Herscovitch, P.; Eckelman, W. C. PET evaluation of [¹⁸F]FCWAY, an analog of the 5-HT1A receptor antagonist, WAY-100635. *Nucl. Med. Biol.* **2000**, *27*, 493–497.

(22) Ma, Y.; Kiesewetter, D. O.; Lang, L.; Der, M.; Huang, B.; Carson, R. E.; Eckelman, W. C. Determination of [¹⁸F]FCWAY, [¹⁸F]FP-TZTP, and their metabolites in plasma using rapid and efficient liquid–liquid and solid-phase extractions. *Nucl. Med. Biol.* **2003**, *30*, 233–240.

(23) Ravert, H. T.; Bencherif, B.; Madar, I.; Frost J. J. PET imaging of opioid receptors in pain: progress and new directions. *Curr. Pharm. Des.* **2004**, *10*, 759–768.

(24) Brodsky, M.; Elliott, K.; Hynansky, A.; Jenab, S.; Inturrisi, C. E. Quantitation of mu-opioid receptor (MOR-1) mRNA in selected regions of the rat CNS. *Neuroreport* **1995**, *6*, 725–729.

(25) Raynor, K.; Kong, H.; Chen, Y.; Yasuda, K.; Yu, L.; Bell, G. I.; Reisine, T. Pharmacological characterization of the cloned κ-, δ-, and μ-opioid receptors. *Mol. Pharm.* **1994**, *45*, 330–334.

(26) Palczewski, K.; Kumasaka, T.; Hori, T.; Behnke, C. A.; Motoshima, H.; Fox, B. A.; Trong, I L.; Teller, D. C.; Okada, T.; Stenkamp, R. E.; Yamamoto, M.; Miyano, M. Crystal structure of Rhodopsin: a G protein-coupled receptor. *Science* **2000**, *289*, 739–745.

(27) (a) Strahs, D.; Weinstein, H. Comparative modeling and molecular dynamics studies of the δ, κ, and μ-opioid receptors. *Protein Eng.* **1997**, *10*, 1019–1038. (b) Pogozheva, I. D.; Lomize, A. L.; Mosberg, H. I. Opioid receptor three-dimensional structures from distance geometry calculations with hydrogen bonding constraints. *Biophys. J.* **1998**, *75*, 612–634. (c) Filizola, M.; Laakkonen, L.; Loew, G. H. 3D modeling, ligand binding, and

activation studies of the cloned δ-, μ, and κ-opioid receptors. *Protein Eng.* **1999**, *12*, 927–942. (d) Zhang, Y.; Sham, Y. Y.; Rajamani, R.; Gao, J.; Portoghese, P. S. Homology modeling and molecular dynamics simulation of the mu opioid receptor in a membrane-aqueous system. *Chem. Bio Chem.* **2005**, *6*, 853–859.

(28) Bissantz, C.; Bernard, P.; Hibert, M.; Rognan, D. Protein-based virtual screening of chemical databases. II. Are homology models of G-protein coupled receptors suitable targets? *Proteins Struct. Funct. Genet.* **2003**, *50*, 5–25.

(29) (a) Okada, T.; Ernst, O. P.; Palczewski, K.; Hofmann, K. P. Activation of rhodopsin: new insights from structural and biochemical studies. *Trends Biochem. Sci.* **2001**, *26*, 318–324. (b) Hubbell, W. L.; Altenbach, C.; Hubbell, C. M.; Khorana, H. G. Rhodopsin structure, dynamics, and activation: a perspective from crystallography, site-directed spin labeling, sulfhydryl reactivity, and disulfide cross-linking. *Adv. Protein Chem.* **2003**, *63*, 243–290.

(30) (a) Peeters, O. M.; Blaton, N. M.; De Ranter, C. J.; van Herk, A. M.; Goubitz, K.; Crystal and Molecular Structure of *N*-[1-(2-phenylethyl)-4-piperidinylium]-*N*-phenylpropanamide (fentanyl) citrate-toluene Solvate. *J. Cryst. Mol. Struct.* **1979**, *9*, 153–161. (b) Flippen-Anderson, J. L.; George, C.; Bertha, C. M.; Rice, K. C. X-ray crystal structures of potent opioid receptor ligands: Etonitazene, *cis*-(+)-3-Methylfentanyl, Etorphine, Diprenorphine, and Buprenorphine. *Heterocycles* **1994**, *39*, 751–766. (c) Brine, G. A.; Stark, P. A.; Liu, Y.; Carroll, F. I.; Singh, P.; Xu, H.; Rothman, R. B. Enantiomers of diastereomeric *cis*-*N*-[1-(2-hydroxy-2-phenylethyl)-3-methyl-4-piperidyl]-*N*-phenylpropanamides: Synthesis, X-ray analysis, and biological activities. *J. Med. Chem.* **1995**, *38*, 1547–1557.

(31) Brine, G. A.; Boldt, K. G.; Huang, P.-T.; Sawyer, D. K.; Carroll, F. I. Carbon-13 nuclear magnetic resonance spectra of fentanyl analogues. *J. Heterocycl. Chem.* **1989**, *26*, 677–686.

(32) (a) Martins, J.; Andrews, P. Conformation-activity relationships of opiate analgesics. *J. Comput.-Aided Mol. Des.* **1987**, *1*, 53–72. (b) Subramanian, G.; Ferguson, D. M. Conformational landscape of selective mu-opioid agonists in gas phase and in aqueous solution: the fentanyl series. *Drug Des. Discovery* **2000**, *17*, 55–67.

(33) The numbering of the human μ receptor corresponds to that of the the rat μ receptor for consistency with mutagenesis data and to allow an easy comparison with the previously reported μ-receptor models.[27]

(34) (a) Surratt, C. K.; Johnson, P. S.; Moriwaki, A.; Seidleck, B. K.; Blaschak, C. J.; Wang, J. B.; Uhl, G. R.m-Opiate receptor: Charged transmembrane domain amino acids are critical for agonist recognition and intrinsic activity. *Biol. Chem.* **1994**, *269*, 20548–20553. (b) Mansour A.; Taylor L. P.; Fine J. L.; Thompson R. C.; Hoversten M. T.; Mosberg H. I.; Watson S. J.; Akil H. Key residues defining the mu-opioid receptor binding pocket: a site-directed mutagenesis study. *J. Neurochem.* **1997**, *68*, 344–353. (c) Li, J. G.; Chen, C.; Yin J.; Rice, K.; Zhang, Y.; Matecka, D.; de Riel, J. K.; DesJarlais, R. L.; Liu-Chen, L. Y. ASP147 in the third transmembrane helix of the rat mu opioid receptor forms ion-pairing with morphine and naltrexone. *Life Sci.* **1999**, *65*, 175–85. (d) Chen, C.; Yin, J.; Riel, J. K.; DesJarlais, R. L.; Raveglia L. F.; Zhu, J.; Liu-Chen, L. Y.; Determination of the amino acid residue involved in [³H]beta-funaltrexamine covalent binding in the cloned rat mu-opioid receptor. *J Biol. Chem.* **1996**, *271*, 21422–21429.

(35) Pogozheva, I. D.; Lomize, A. L.; Mosberg, H. I. Opioid Receptor Three-dimensional Structures from Distance Geometry Calculations with Hydrogen Bonding Constraints. *Biophys. J.* **1998**, *75*, 612–634.

(36) Tang, Y.; Chen, K. X.; Jiang, H. L.; Wang, Z. X.; Ji, R. Y.; Chi, Z. Q. Molecular Modeling of the μ-Opioid Receptor and its Interaction with OHMefentanyl. *Acta Pharmacol. Sin.* **1996**, *17*, 156–160.

(37) Xu, H.; Lu, Y.-F.; Partilla, J. S.; Zheng, Q.-X.; Wang, J.-B.; Brine, G. A.; Carroll, I.; Rice, K. C.; Chen, K.-X.; Chi, Z.-Q.; Rothman, R. B. Opioid Peptide Receptor Studies, 11: Involvement of Tyr148, Trp318, and His319 of the Rat μ-Opioid Receptor in Binding of μ-Selective Ligands. *Synapse* **1999**, *32*, 23–28.

(38) Ulens, C.; Van Boven, M.; Daenens, P.; Tytgat, J.; Interaction of *p*-fluorofentanyl on cloned human opioid receptors and exploration of the role of Trp-318 and His-319 in mu-opioid receptor selectivity. *J. Pharmacol. Exp. Ther.* **2000**, *294*, 1024–1033.

(39) Shi, L.; Liapakis, G.; Xu, R.; Guarnieri, F.; Ballesteros, J. A.; Javitch, J. A. α-2-adrenergic receptor activation. Modulation of the proline kink in transmembrane 6 by a rotamer toggle switch. *J. Biol. Chem.* **2002**, *277*, 40989–40996.

(40) Mouledous, L.; Topham, C. M.; Moisand, C.; Mollereau, C.; Meunier, J. C. Functional inactivation of the nociceptin receptor by alanine substitution of glutamine 286 at the C terminus of transmembrane segment VI: evidence from a site-directed mutagenesis study of the ORL1 receptor transmembrane-binding domain. *Mol. Pharmacol.* **2000**, *57*, 495−502.

(41) Subramanian, G.; Paterlini, M. G.; Portoghese, P. S.; Ferguson, D. M. Molecular Docking Reveals a Novel Binding Site Model for Fentanyl at the μ-Opioid Receptor. *J. Med. Chem.* **2000**, *43*, 381−391.

(42) (a) Henriksen, G.; Platzer, S.; Schütz, J.; Schmidhammer, H.; Rafecas, M. L.; Schwaiger, M.; Wester, H.-J. 2003. ^{18}F-fluorinated agonists and antagonists for imaging of μ-opioid receptors: Approaches to ^{18}F-carfentanil, ^{18}F-sufentanil and ^{18}F-cyprodime. *J. Labeld. Compds. Radiopharm.* **2003**, *46*, S175. (b) Henriksen, G.; Herz, M.; Schwaiger, M.; Wester, H.-J. Synthesis of ^{18}F-fluoroalkyl esters of Carfentanil. *J. Labelled Compds. Radiopharm.* **2005**, *48*, 1−9.

(43) Dolbier, W. R.; Lee, S. K.; Phanstiel, O. The in situ generation and trapping of some fluorine substituted ketenes. *Tetrahedron* **1991**, *47*, 2065−2072.

(44) Guhlke, S.; Coenen, H. H.; Stöcklin, G. Fluoroacylation agents based on small nca [^{18}F]fluorocarboxylic acids. *Appl Radiat. Isot.* **1994**, *6*, 715−727.

(45) Morris, G. M.; Goodsell, D. S.; Halliday, R. S.; Huey, R.; Hart, W. E.; Belew, R. K.; Olson, A. J. Automated docking using a Lamarckian genetic algorithm and an empirical binding free energy function. *J. Comput. Chem.* **1998**, *19*, 1639−1662.

(46) SYBYL Molecular Modeling System (version 6.8), TRIPOS Assoc., St. Louis, MO.

(47) Head, J.; Zerner, M. C. A Broyden-Fletcher-Goldfarb-Shannon optimization procedure for molecular geometries. *Chem. Phys. Lett.* **1985**, *122*, 264−274.

(48) Gasteiger, J.; Marsili, M. Iterative partial equalization of orbital electronegativity−a rapid access to atomic charges. *Tetrahedron* **1980**, *36*, 3219−3228.

(49) Waterhouse, R. N. Determination of lipophilicity and its use as a predictor of blood-brain barrier penetration of molecular imaging agents. *Mol. Imag. Biol.* **2003**, *5*, 376−389.

(50) Henriksen, G.; Platzer, S.; Hauser, A.; Willoch, F.; Berthele, A.; Schwaiger, M.; Wester, HJ. ^{18}F-labeled sufentanil for PET-imaging of mu-opioid receptors. *Bioorg. Med. Chem. Lett.* **2005**, *15*, 1773−1777.